Design, synthesis and biological evaluation of quinazoline derivatives as anti-trypanosomatid and anti-plasmodial agents

ARTICLE *in* EUROPEAN JOURNAL OF MEDICINAL CHEMISTRY · MAY 2015

Impact Factor: 3.45 · DOI: 10.1016/j.ejmech.2015.04.028

European Journal of Medicinal Chemistry 96 (2015) 296–307

Contents lists available at ScienceDirect

European Journal of Medicinal Chemistry

journal homepage: http://www.elsevier.com/locate/ejmech

Original article

Design, synthesis and biological evaluation of quinazoline derivatives as anti-trypanosomatid and anti-plasmodial agents

César Mendoza-Martínez [a, b], José Correa-Basurto [c], Rocío Nieto-Meneses [d], Adrián Márquez-Navarro [d], Rocío Aguilar-Suárez [d], Miriam Dinora Montero-Cortes [d], Benjamín Nogueda-Torres [d], Erick Suárez-Contreras [d], Norma Galindo-Sevilla [e], Ángela Rojas-Rojas [f], Alejandro Rodriguez-Lezama [f], Francisco Hernández-Luis [a, b, *]

[a] Programa de Maestría y Doctorado en Ciencias Químicas, UNAM, México, DF 04510, Mexico
[b] Facultad de Química, Departamento de Farmacia, UNAM, México, DF 04510, Mexico
[c] Escuela Superior de Medicina, Laboratorio de Modelado Molecular y Bioinformática de la SEPI, IPN, México, DF 11340, Mexico
[d] Escuela Nacional de Ciencias Biológicas, Departamento de Parasitología, IPN, México, DF 11340, Mexico
[e] Departamento de Infectología, Instituto Nacional de Perinatología, México, DF 11000, Mexico
[f] Tecsiquim S.A. de C.V., Toluca Estado de México 50233, Mexico

ARTICLE INFO

Article history:
Received 20 November 2014
Received in revised form
10 April 2015
Accepted 11 April 2015
Available online 14 April 2015

Keywords:
Trypanosoma cruzi
Leishmania mexicana
Plasmodium berghei
Quinazoline
Dihydrofolate reductase
Pteridin reductase

ABSTRACT

In this paper, the design, synthesis and biological evaluation of a set of quinazoline-2,4,6-triamine derivatives (**1**–**9**) as trypanocidal, antileishmanial and antiplasmodial agents are explained. The compounds were rationalized basing on docking studies of the dihydrofolate reductase (DHFR from *Trypanosoma cruzi*, *Leishmania major* and *Plasmodium vivax*) and pteridin reductase (PTR from *T. cruzi* and *L. major*) structures. All compounds were in vitro screened against both bloodstream trypomastigotes of *T. cruzi* (NINOA and INC-5 strains) and promatigotes of *Leishmania mexicana* (MHOM/BZ/61/M379 strain), and also for cytotoxicity using Vero cell line. Against *T. cruzi*, three compounds (**5**, **6** and **8**) were the most effective showing a better activity profile than nifurtimox and benznidazole (reference drugs). Against *L. mexicana*, four compounds (**5**, **6**, **8**, and **9**) exhibited the highest activity, even than glucantime (reference drug). In the cytotoxicity assay, protozoa were more susceptible than Vero cells. In vivo *Plasmodium berghei* assay (ANKA strain), the compounds **1**, **5**, **6** and **8** showed a more comparable activity than chloroquine and pyrimethamine (reference drugs) when they were administrated by the oral route. The antiprotozoal activity of these substances, endowed with redox properties, represented a good starting point for a medicinal chemistry program aiming for chemotherapy of Chagas' disease, leishmaniosis and malaria.

1. Introduction

Parasitic infectious diseases due to pathogenic protozoan still constitute a major health problem world wide and mainly occur in underdeveloped countries [1]. Chagas' disease (CD), caused by *Trypanosoma cruzi* [2], leishmaniosis, caused by *Leishmania* spp. [3], and malaria, caused by *Plasmodium vivax* and *Plasmodium falciparum* [4], are among the most serious infections in the tropical regions. CD is broadly disperse in Latin America and the Caribbean region, affecting approximately 8 million people, of whom 30–40% either have or will develop cardiomyopathy, digestive megasyndromes, or both [2]. Leishmaniosis are endemic in 98 countries or territories with an estimated incidence of 0.2–0.4 million cases of visceral leishmaniosis (VL) and 0.7–1.2 million cases of cutaneous leishmaniasis (CL) each year [5]. The clinical manifestations may vary from single cutaneous lesions to fatal VL [3,5]. Meanwhile, malaria remains in large areas of the developing world, with 40% of the earth's population living in malaria-endangered areas. As a direct consequence, over 1 million humans per year die of this disease, with the estimate of 550 million clinical cases [4]. These public health problems are accentuated by multiple factors including the AIDS epidemic, the increase of international travel and difficulties controlling vectors.

* Corresponding author. Facultad de Química, Departamento de Farmacia, UNAM, México, DF 04510, Mexico.
E-mail address: franher@unam.mx (F. Hernández-Luis).

http://dx.doi.org/10.1016/j.ejmech.2015.04.028
0223-5234/

In the absence of effective vaccines, chemotherapy plays a critical role controlling these diseases [1,6]. The treatment of CD relies on two available drugs; nifurtimox (**Nfx**, Lampit™) and benznidazole (**Bnz**, Rochagan™), introduced into the clinical therapy over four decades ago. Although in most cases these drugs are efficient in the acute phase of the disease, they are almost ineffective in the chronic phase [7]. For the treatment of leishmaniosis, glucantime, miltefosine and amphotericine B, are in use to date; however, these compounds have common drawbacks such as high toxicity, high cost or emerging resistance [8]. Regarding malaria, sulfadoxine–pyrimethamine, quinine, chloroquine and their derivatives, are still in use today; new therapies based on artemisinin were recently introduced into the clinic [9]. Moreover, the emergences of drug-resistant strains of the causative organisms have seriously impaired their therapeutic value. This has frustrated attempts to eradicate these diseases by means of chemotherapy, and the currently used drugs have an increased risk of becoming obsolete. In this context, intensive efforts have been devoted to find novel prototype compounds among natural and synthetic sources to develop new drugs to treat these infectious diseases.

In previous research work using quinazoline-2,4,6-triamine (**TAQ**) as template, Davoll et al. [10] synthesized a series of derivatives bearing different substituents at the 6-position. Several compounds displayed strong antiparasitic activity against *Plasmodium berghei*, and modest activity against *T. cruzi* in cultures of chicken embryo cells and in mice, respectively. Subsequently, other studies showed the ability of **TAQ** to co-crystallize with pteridine reductase 1 of *Leishmania major* (lmPTR1) [11] and that several quinazoline-2,4-diamine derivatives had the ability to interact with dihydrofolate reductase (DHFR) isolated from *Leishmania mexicana* (lmxDHFR) and *T. cruzi* (tcDHFR) [12,13]. PTR1 and DHFR are implicated in the metabolism of folate parasitic protozoa, and they are treatable targets for antiparasitic leads [8]. In addition, it is known that the mechanism of antifolate resistance in *L. major* and *T. cruzi* is mediated by PTR and its isoforms [14,15].

The sum of these results encouraged the further search for other **TAQ** derivatives as trypanocidal, antileishmanial and antiplasmodial agents. In this context, this document presents the design and synthesis of nine quinazoline derivatives (**1**–**9**, Table 1) with their in vitro evaluation against bloodstream trypomastigotes of *T. cruzi* (NINOA and INC-5 strains) and promastigotes of *L. mexicana* (MHOM/BZ/61/M379 strain). Likewise, compounds were evaluated in *P. berghei* mouse model of infection.

The design was conducted searching the best ligand arrangement into tcDHFR, lmDHFR, pvDHFR, tcPTR2 and lmPTR1.

2. Results and discussion

2.1. Design

The quinazoline derivative **1** showed a good profile against *T. cruzi* and *P. berghei* in previous studies [10]. In order to know the factors for this behavior, the theoretical interaction of this compound with tcDHFR and tcPTR2 (Fig. 1) was analyzed.

According to the molecular docking of **1** with both proteins, three regions with different characteristics were found in tcDHFR and two in tcPTR2. Similar findings were presented with lmDHFR, pvDHFR, hDHFR, and lmPTR1 (Table 2). Into DHFR, region I present a lipoid character because it is constituted by alkyl and aromatic side chains. Region II has got a hydrophilic character mainly formed by hydrophilic amino acids, CO and NH groups of the peptide bonds. Region III has got arginine capable of bridging hydrogen with the 4-methoxy substituent of **1**. The three regions are present in DHFR for both, human and parasite; however, they strongly differ in region I, where the parasite proteins have got an aromatic ring (Phe or Tyr) whereas the human protein is more hydrophilic (Asn64). Selective parasite protein compounds should be directed primarily towards region I. The best interaction of **1** with DHFR or PTR is with region I. On the other hand, **TAQ** moiety interacts with the previously reported aminoacids [11,13].

Table 1
Quinazoline derivatives.

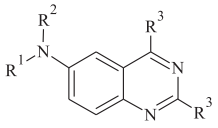

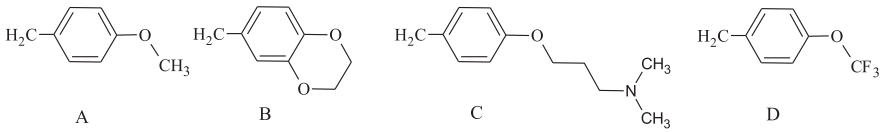

Compound	R^1	R^2	R^3	MW	Mp (°C)	Clog P[a]	HBD[b]	HBA[c]	PSA (Å^2)[d]
1	A	H	NH_2	295	215–216	2.24	5	6	99.09
2	A	H	$NHCOCH_3$	371	187–188	2.13	3	8	105.24
3	B	H	NH_2	323	134–136	1.61	5	7	108.33
4	C	H	NH_2	366	198–200	2.54	5	7	102.33
5	D	H	NH_2	349	206–207	3.15	5	6	99.09
6	D	Ethyl	NH_2	377	177–178	3.77	4	6	90.30
7	A	A	NH_2	415	106–107	3.94	4	7	99.54
8	A	D	NH_2	469	121–122	4.85	4	7	99.54
9	D	D	NH_2	523	133–135	5.76	4	7	99.54

[a] Calculated from molinspiration (www.molinspiration.com).
[b] HBA: Hydrogen bond-acceptor group.
[c] HBD: Hydrogen bond-donor group.
[d] PSA: Polar surface area.

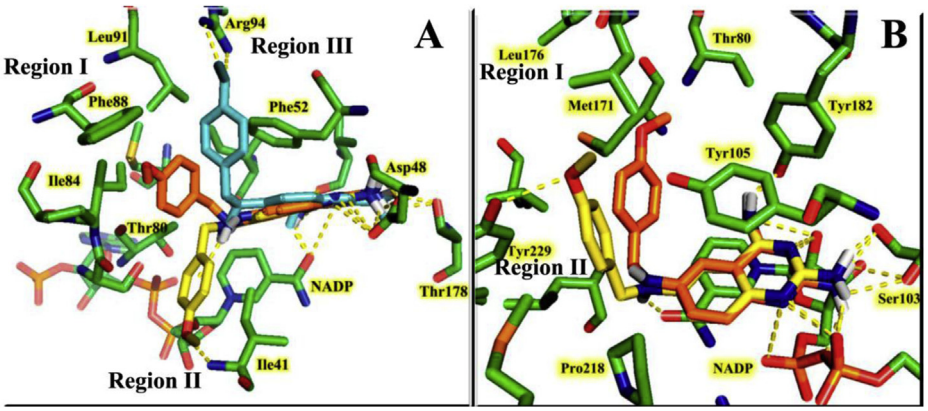

Fig. 1. Poses and interactions of compound **1** on A) tcDHFR and B) tcPTR2.

With this in mind, new derivatives were designed in order to replace the 4-methoxy substituent of **1** considering the predicted interactions for docking studies. Generally, **3**–**5** compounds contain lyphophilic substituents at 6-position in order to bring their association with target enzymes. Additionally, compound **5** was designed to prevent the metabolism by *O*-dealkylation, replacing 4-methoxy group by 4-trifluoromethoxy group (Fig. 2) and removes the density of the oxygen electron decreasing the ability to bridge hydrogen with regions II and III, in order to increase the selectivity towards the parasite proteins by preferentially interacting with region I.

Compounds **6**–**9** were designed to interact with two regions in the proteins. Docking analyses under DHFR and PTR show that the hypothesis is correct, and that the two N^6substituents are primarily directed toward regions I and II (Fig. 3).

2.2. Chemistry

The compounds mentioned above (**1**–**5**) were synthesized according to the sequence of reactions outlined in Scheme 1. The cyclocondensation of commercial 5-nitroanthranilonitrile (**10**) with guanidine hydrochloride led to 6-nitroquinazoline-2,4-diamine (**11**); which was treated with acetic anhydride followed by hydrogenation under a hydrogen atmosphere using palladium on charcoal to furnish *N*,*N*′-(6-aminoquinazoline-2,4-diyl)diacetamide (**12**). Subsequent condensation of **14** with substituted benzaldehydes and reduction with sodium borohydride ($NaBH_4$) gave **1**, **3**–**5**, respectively. The synthesis of compound **2** also took place via reductive amination, however, the synthesis conditions were different. In this case, both solvent and temperature were modified because the acetyl group loses when this reaction is carried out in methanol.

For compounds **6**–**9**, **1** and **5** were used, which were condensed with the corresponding aldehyde under acidic conditions. Two different reducing agents were used, for **6**, sodium cyanoborohydride ($NaBH_3CN$), and for **7**–**9**, sodium triacetoxyborohydride [$NaBH(OAc)_3$] (Scheme 2).

Target compounds **1**–**9** were obtained in fair yields and pure as solids with sharp melting points (Table 1). The structures of the synthesized compounds were confirmed by spectroscopic techniques, such as ^{1}H NMR, ^{13}C NMR, infrared, TOF mass spectra and FAB mass spectra or elemental analyses.

All compounds have signals in common due to similar functional groups in both IR and NMR spectra. The ^{1}H NMR of amine group, in 2-position, was found at 5.6 ppm for compounds **1** and **3**–**6**, and approximately 6–7 ppm for compounds **7**–**9**. The amine group, in 4-position, is approximately 7 ppm for compounds **1** and **3**–**6** and 7–8 ppm for compounds **7**–**9**. Curiously, the substitution degree is associated with amines' displacement. For the acetylated compound **2**, there are not any present amines, and NH groups (amides) are at a lower field (10–11 ppm). In addition, the amine in 6-position only exists in compounds **1**–**5** and this occurs as a triplet at approximately 5.6 ppm.

Table 2
Analysis of interactions for compound **1** with DHFR and PTR.

Protein	Region I (hydrophobic)	Region II (hydrophilic)	Region III (hydrophilic)	TAQ interactions
lmDHFR	Trp84, Val87, Phe91, Leu94, and Val101	Glu43, Ser44, Ser86 (hydrogen bond with methoxy group) and cofactor NADP	Arg97 (hydrogen bond with methoxy group)	Val30, Phe56 (¶-stacking), Asp52, Val156, Thr180 and cofactor NADP (nicotinamide moiety)
lmPTR1	Met183, Leu188, Leu226, Tyr283	Leu229, Val230 (hydrogen bond with methoxy group), Asp232		Ser 111, Phe113 (¶-stacking), Tyr194 and cofactor NADP (¶-stacking-nicotinamide moiety and hydrogen bond-phosphate group)
tcDHFR	Ile84, Pro85, Phe88, and Leu91	Ile41 (hydrogen bond with methoxy group), Ser83, and cofactor NADP	Arg94 (hydrogen bond with methoxy group)	Val26, Phe52 (¶-stacking), Asp48 Ile154, Thr178 and cofactor NADP (nicotinamide moiety)
tcPTR2	Met171, Leu176, Leu214	Leu 217, Met221, Tyr229 (hydrogen bond with methoxy group), and Pro218		Ser103, Tyr105 (¶-stacking), Tyr182 and cofactor NADP (¶-stacking-nicotinamide moiety and hydrogen bond-phosphate group)
pvDHFR	Trp118, Ile121, Pro122, Tyr125, Leu128	Gly43, Leu45 and cofactor NADP	Arg131 (hydrogen bond with methoxy group)	Ile13, Cys14, Asp53, Ile173, Tyr179,Thr194, Phe57 (¶-stacking) and cofactor NADP (nicotinamide moiety)
hDHFR	Trp57, Ile60, Pro61, Asn64, Leu67	Asp21, Leu22 and cofactor NADP	Arg70 (hydrogen bond with methoxy group)	Val115, Tyr121, Ile7, Phe34 (¶-stacking), Glu30 and cofactor NADP (nicotinamide moiety)

Fig. 2. Replacing the methoxy group of compound **1** for trifluoromethoxy group.

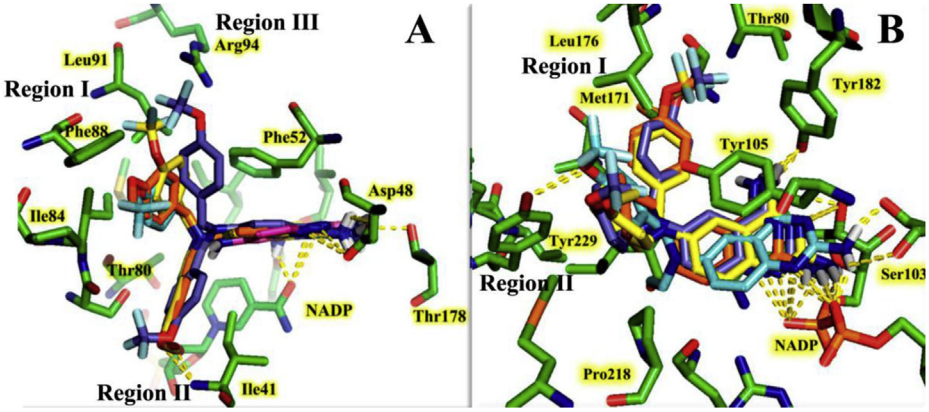

Fig. 3. Interaction of compounds **6**–**9** (green: **6**, orange: **7**, yellow: **8**, purple: **9**) on A) tcDHFR and B) tcPTR2. (For interpretation of the references to colour in this figure legend, the reader is referred to the web version of this article.)

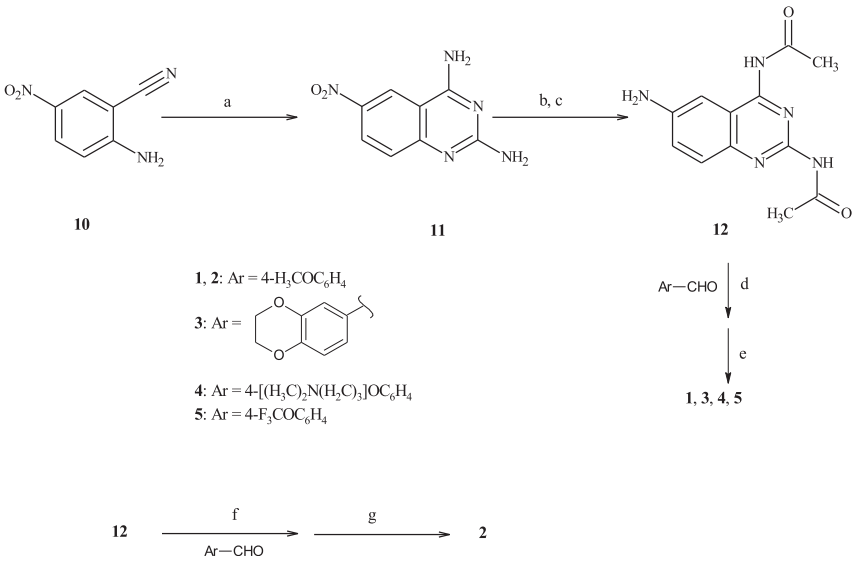

Scheme 1. Reagents and conditions: (a) guanidine hydrochloride, NaOH, EtOH/PrOH, reflux; (b) acetic anhydride, 110 °C; (c) H_2, 10% Pd/C, MeOH, r.t.; (d) MeOH, 60 °C, 1 h; (e) 0 °C, $NaBH_4$;(f) DMF, 85 °C, 1 h; (g) 0 °C, $NaBH_4$.

The methyl protons in compounds **1**–**2** and **8**–**9** are at approximately 3.7 ppm in ^{1}H NMR and 55 ppm in ^{13}C NMR. The methylene group protons linking the quinazoline nucleus with benzyl groups are approximately at 4 ppm as doublets in compounds **1**–**5**, and as singlets, slightly displaced downfield (4.5 ppm), for compounds **6**–**9**. This signal in ^{13}C NMR is of 46 ppm for compounds **1**–**6** and 53 ppm for compounds **7**–**9**. Interestingly, compound **8** has got two different substituents (*p*-methoxybenzyl and *p*-trifluoromethoxybenzyl) and there are two methylene signals; in both ^{1}H and ^{13}C NMR they are very close together. On the other hand, the CF_3 group signal is approximately 120 ppm and appears as a quartet with a large *J* (above 257 Hz) in all derivatives with fluorine atom.

2.3. Antiprotozoal in vitro activity

The compounds **1**–**9** were tested in vitro against bloodstream trypomastigotes of two *T. cruzi* strains (NINOA and INC-5) (Table 3). Anti-*T. cruzi* properties were expressed in terms of the LC_{50} (50% lytic concentration) for each compound. This parameter was calculated after 24 h of parasite exposition. **Nfx** and **Bnz** were used as reference drugs. In general, most compounds were more active than the reference drug. First, as can be seen in data of Table 3, the NINOA strain was more susceptible to compound **5**, **6** and **8** (LC_{50}: 6.42, 20.56 and 17.77 μM, respectively). The INC-5 strain was more susceptible to compound **9** (LC_{50}: 29.23 μM) and then to

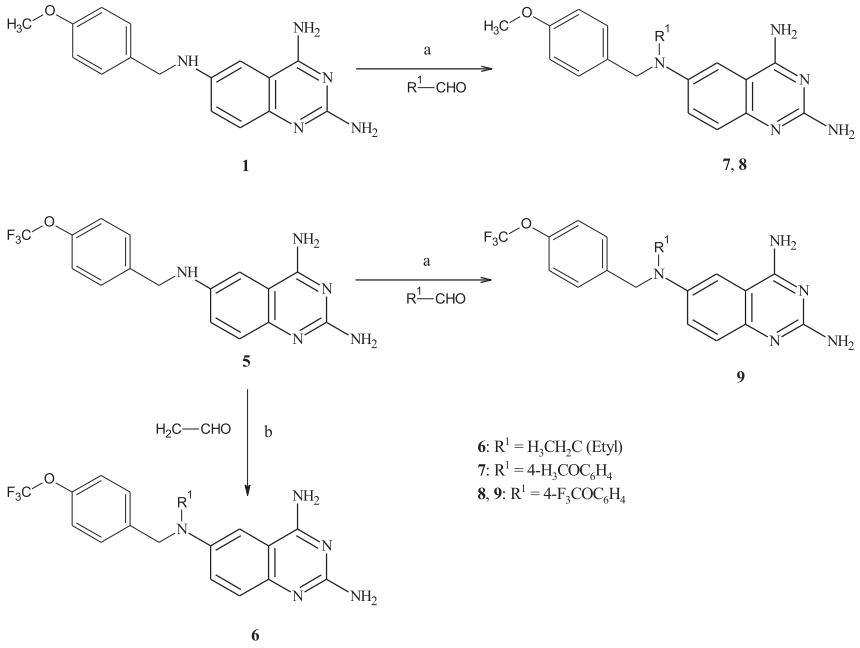

Scheme 2. Reagents and conditions: (a) CH_3CN/CH_3COOH (1:1), $NaBH(OAc)_3$; (b) CH_3CN, $NaBH_3CN$ then HCl (38%).

Table 3
In vitro activity of **1**–**9** against bloodstream trypomastigote of *T.cruzi* and promatigotes of *L. mexicana*.

Compound	*Trypanosoma cruzi*		*Leishmania mexicana*
	NINOA strain	INC-5 strain	MHOM/BZ/61/M379 strain
	LC_{50} (μM) ± SD	LC_{50} (μM) ± SD	LC_{50} (μM) ± SD
1	32.74 ± 3.40	155.00 ± 4.78	14.59 ± 1.32
2	196.89 ± 6.71	508.61 ± 12.32	250.00 ± 3.56
3	66.51 ± 3.98	72.47 ± 13.71	22.35 ± 2.73
4	287.81 ± 16.54	183.67 ± 7.61	65.43 ± 6.45
5	20.56 ± 3.37	46.06 ± 7.59	8.08 ± 3.18
6	6.28 ± 0.65	43.82 ± 8.96	3.06 ± 1.80
7	62.64 ± 0.27	46.52 ± 4.53	23.10 ± 1.42
8	17.77 ± 0.79	40.67 ± 8.96	8.00 ± 0.89
9	35.01 ± 4.21	29.23 ± 6.34	4.93 ± 0.52
Glucantime	nd	nd	182.68 ± 0.19
Nfx	600 ± 18.92	310 ± 9.45	nd
Bnz	780 ± 12.23	690 ± 6.78	nd

nd: not determined.
LC: lytic concentration.
SD: Standard deviation.

compounds **5**, **6** and **8**. Second, compounds **1**, **2**, **3** and **4** exhibited low activity towards both strains. Compound **4** was the least active with LC_{50} above 200 μM.

The activity against *L. mexicana* had a similar tendency to those obtained against *T. cruzi* (Table 3). The most active compounds were **5**, **6**, **8** and **9**. Compound **6** had the lowest LC_{50}, indicating that the activity had increased. Compound **2** was the least active with LC_{50} of 250 μM.

Globally considered, the potency in both parasites is as follows: **6** > **5**>**9** > **8**>**1** > **7**>**3** > **2**>**4**. The variations of this order may be due to genetic factors, virulence factors or analysis conditions.

Due to the small number of evaluated compounds, the attempt of analyzing SAR aspects seems unreasonable, but several observations and comparisons on the results can be made. The most active compounds are those with fluorine atoms, which could indicate an effect of lipophilicity. However, it is not the only factor because, the compound with the highest value of clogP (compound **9**), does not have the best biological activity. Some other factors to consider could be steric or electronic. Compound **6** has an ethyl as second substituent on the N^6 position, and it is the most active against *T. cruzi* (NINOA strain) and *L. mexicana*; when increasing the size of the substituent to an aromatic ring (**7**, **8** and **9**) the activity decreases, indicating the influence of the steric factor. The substitution of amines groups, at 2 and 4-position, for acetamides (**2**) decreases their biological activity, which means that they are very important for the interaction with its receptor. Compound **4** was the least active, which could be due to the size of the substituent in the benzene ring. However, this substituent may not have an electronic effect on the quinazoline nucleus and the decreased activity is due only to size.

2.4. In vitro cytotoxicity studies

An important criterion in the search of active compounds with antiprotozoal activity is their toxicity on mammalian host cells. For this purpose, the cytotoxicity was determined using Vero cells and expressed as the concentration required to kill 50% of the mammalian cells (CC_{50}). The quinazoline derivatives were evaluated and the CC_{50} was determined. In this work, compounds with CC_{50} < 100 μM were classified as toxic for the mammalian cell line. With this criterion, none of the compounds was toxic for mammalian cells (Table 4).

2.5. In vivo antiplasmodial activity

In vivo activity of quinazolines derivatives on *P. berghei* murine model was evaluated. For the *P. berghei* murine model, the compounds were applied at 0–4 days post-inoculation (pi) and they were dosed by oral route at a dose of 50 mg/kg during 4 days. Data showed that compounds **1**, **5**, **6** and **8** were the most active in the parasitemia reduction (98.5, 99.9, 100 and 95.2%, respectively) (Table 5). These compounds showed almost the same activity as the positive controls, chloroquine (**CQ**) and pyrimethamine (**Pyr**). No discernible toxic side effects in the mice were associated with any of the compounds. Compound **2** was a little bit less active (89.3%),

while the other quinazoline derivatives (**4**, **7** and **9**) showed a very weak or nonexistent activity (**3**).

2.6. ABTS assay

A study of the antioxidant capacity of the compounds as an indicator of the modification of the electron distribution in molecules was performed. Results are presented as the ability of compounds to scavenge 50% of free radical $ABTS^{\bullet+}$ (IC_{50}) (Table 6). The order of antiradical activity is as follow: **5** > **3**>**4** > **1**>**TAQ**>**6** > **8**>**9** > **7**. Interestingly, the highest antiradical power, which is compound **5**, is one of the most active against *T. cruzi*, *L. mexicana* and *P. berghei*. Compounds **1**, **3** and **4** have got a slightly lower antiradical capacity. This indicates that the influence of the substituent in the benzene ring is hardly perceived in the quinazoline nucleus. The disubstituted compound **6**, has got a lower radical scavenging effect to the above compounds, in this case, the influence of the second substituent is remarkable. However, there are many more differences to those who are disubstituted by two aromatic rings (**7**, **8** and **9**) with IC_{50} values that are much lower. That there is no obvious correlation of these results with the biological activity, could indicate that the electronic requirements are not as important as the steric effect or lipophilicity (change due to fluorine atom), but still more work is needed in order to try this hypothesis.

2.7. Exploratory DHFR inhibition

In this study, only two of the most active compounds (**5** and **6**) were analyzed. Folic acid and folinic acid studies were carried out to explore the participation of DHFR inhibition on antiparasitic activity of **5** or **6**. Folic acid is an essential co-factor for the enzyme DHFR involved in the de-novo synthesis of purines and pyrimidines, the essential precursors of DNA. Folinic acid is the reduced form of folic acid that circumvents the inhibition of DHFR, so some normal DNA replication processes can proceed even in the presence of DHFR inhibitor. For these studies, *L. mexicana* cultures were pretreated with folic acid in order to reduce the interaction of test compound with DHFR; if DHFR inhibition is involved, a decrease in the antiparasitic activity of **5** and **6** should be observed. Additionally, pretreatment with folinic acid provides tetrahydrofolates intracellular and effectively bypasses the block on DHFR induced by test compounds slowing their biological activity. Therefore, if the mechanism of antiparasitic action involves the DHFR inhibition, there must be a clear correlation in the responses of folic and folinic acid studies. Finally, an antioxidant (ferulic acid) was also used with the intention of determining if there is a redox type mechanism involved, this will be obvious by presenting a decrease in the leishmanicidal activity of the quinazoline derivatives.

Table 4
Cytotoxicity activities.

Compound	CC_{50} (μM) ± SD
1	147 ± 3
2	156 ± 8
3	>200
4	>200
5	182 ± 7
6	>200
7	>200
8	>200
9	>200
Nfx	163 ± 3
Pyr	122 ± 4

CC: Cytotoxic concentration.
SD: Standard deviation.

Table 5
In vivo activity of **1**–**3**, **5**–**6**,**8** in *P. berghei* murine models.

Compound	Parasitemia suppression (%)	Survival time (days post-administration)
1	98.5	18 ± 5
2	89.3	6 ± 2
3	44.2	11 ± 3
4	53.2	12 ± 4
5	99.9	17 ± 6
6	100	>23
7	0	7 ± 1
8	95.2	21 ± 1
9	21	14 ± 2
CQ	100	>23
Pyr	100	>23
Control	0	0

Table 6
IC_{50} from ABTS assay.

Compound	IC_{50} (μM)
1	5.72 ± 0.03
2	7.04 ± 0.09
3	6.29 ± 0.17
4	6.38 ± 0.57
5	4.75 ± 0.06
6	7.36 ± 0.13
7	113.95 ± 10.86
8	24.46 ± 0.22
9	33.91 ± 0.54
TAQ	6.78 ± 0.10
Trolox	10.92 ± 0.26
Vitamin C	11.25 ± 0.32
Vitamin E	14.84 ± 0.25

IC: Inhibitory concentration.

It is observed that the antiparasitic activity ameliorates with respect to increasing the concentration of folic acid, folinic acid and ferulic acid. In this sense, it is interesting to note that compound **6** is more dependent on the concentration of these molecules compared to compound **5**. The data also indicates that there is a significant correlation between the data obtained for folic acid and folinic acid, this means that there is a inhibition of DHFR. Besides, the influence of the concentration of ferulic acid on antiparasitic activity indicates the presence of a redox mechanism of action (Fig. 4).

3. Conclusions

We have synthesized, via simple and straightforward routes, nine quinazoline antiparasitic derivatives as potential trypanocidal, leishmanicidal and antiplasmodial agents. Our results indicate that, despite their significant activity against *P. berghei*, the bloodstream trypomastigotes of *T. cruzi* and amastigotes of *L. mexicana*, compounds **5**, **6**, **8** and **9** were the most active compounds compared to compound **1**, which means that rational changes were accurate to increase biological activity. On the other hand, it is important to note that fluoride conferred increased biological activity to the compounds **5**, **6**, **8** and **9**, this is probably because the lipophilicity of the molecule is increased, which modifies its absorption. Data also indicates that the amines groups, at 2 and 4-positions, are important for biological activity and that the activity is lost when acetamides are placed in those positions.

In the case of the possible mechanism of action according to the theoretical results and the experimental data with folic acid, folinic acid and ferulic acid, inhibition of DHFR is proposed but also a redox mechanism could be possible, such as inhibition of PTR or oxidation of molecules to generate a more active metabolite as demonstrated

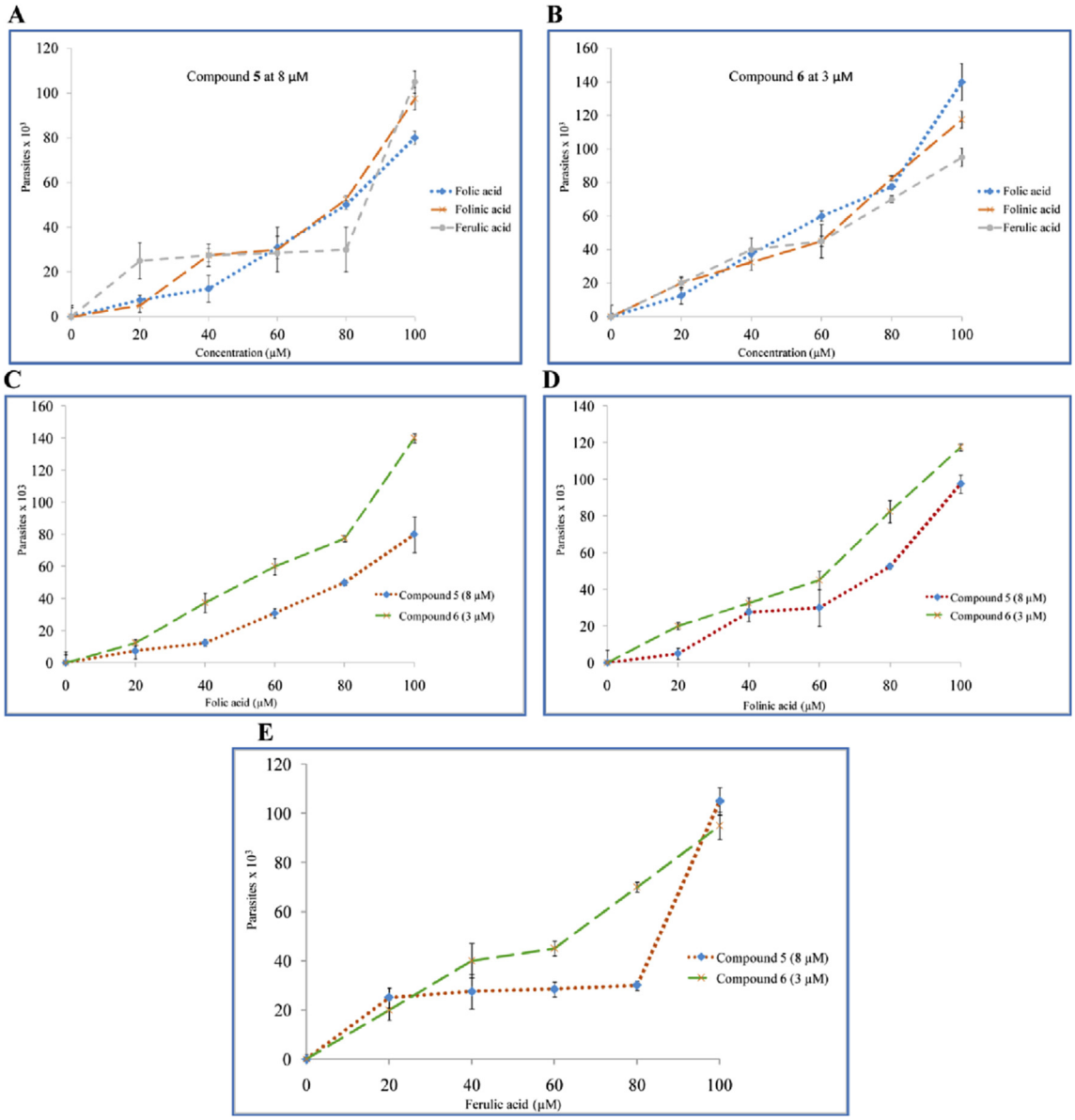

Fig. 4. Effect of different concentrations of folic acid, folinic acid and ferulic acid on the leishmanicidal activity of compounds **5** and **6** (A and B respectively). Comparison of the same effects between **5** and **6** in separate graphs at different concentrations of folic acid (C), folinic acid (D) and ferulic acid (E).

in the ABTS assay. A direct enzymatic study should be conducted to clarify this hypothesis.

Additionally, given the in vitro activity of the compounds as antiprotozoal, an in vivo study should be carried out to *T. cruzi* and *L. mexicana*. In the case of *P. berghei*, dose–response and toxicity in vivo studies are the next step. This study provides a simple modification to an antiparasitic molecule reported by rational design. This is important to progress in the fight against orphan diseases around the world due to the urgency of new treatments for resistant strains.

4. Experimental

4.1. Synthesis

Melting points were determined in open capillary tubes with a Büchi B-540 melting point apparatus and are uncorrected. Reactions were monitored by TLC on 0.2 mm pre-coated silica gel 60 F254 plates (E. Merck) with visualization by irradiation with a UV lamp. Silica gel 60 (70–230 mesh) was used for column chromatography. IR spectra were recorded with an FT Perkin Elmer 16 PC spectrometer. ^{1}H (300 MHz) and ^{13}C (75 MHz) NMR spectra were measured at room temperature using a Varian EM-390 spectrometer. Solvents are indicated in the text. Data for ^{1}H NMR spectra are reported as follows: chemical shifts are given in ppm relative to tetramethylsilane (Me_4Si, $\delta = 0$); J values are given in Hz; splitting patterns have been designated as follows: s, singlet; d, doublet; q, quartet; dd, doublet of doublet; t, triplet; m, multiplet; bs, broad singlet. Data for ^{13}C NMR is reported in terms of chemical shift (δ, ppm) relative to residual solvent peak. MS were recorded on a JEOL JMS-SX102A spectrometer by FAB [FAB(+)] and Water Synapt G2Sspectrometer by TOF MS ES +. Elemental analyses (C, H, N) for new compounds were performed on Fisons EA 1108 instruments and agreed with the proposed structures within ±0.4% of the theoretical values. Catalytic hydrogenations were carried out in a Parr shaker hydrogenation apparatus. Starting materials 5-

nitroanthranilonitrile, aldehydes, NaBH4, $NaBH_3CN$, $NaBH(OAc)_3$ and guanidine hydrochloride were commercially available (Sigma Aldrich).

4.1.1. Synthesis de compounds **1**, **3**–**5**

A solution of appropriate aldehyde (1.60 mmol) and compound **12** (0.4558 g, 1.76 mmol), in methanol (80 ml) was stirred at 60 °C for 2 days. Then the mixture was cold to 0 °C and $NaBH_4$ (0.11 g, 3.20 mmol) was added. Later, it was stirred at room temperature for 12 h. After the mixture was evaporated on rotavapour under decrease pressure and cold water was poured above it. The solid was filtered off, washed with cold water and dried.

4.1.2. N^6-(4-Methoxybenzyl)quinazoline-2,4,6-triamine (**1**)

Yellow powder (0.19 g, 40%, Mp: 215.1–216.8 °C). TLC ($CHCl_3$/MeOH = 80/20) R_f = 0.73. IR (KBr): 3450 and 3328 (N–H), 1639 (C–N), 1469 and 1563 (C=C Ar), 1243 (C–O–C); ^{1}H NMR (DMSO-d_6) ppm: 3.72 (s, 3H, CH_3), 4.20 (d., J = 6, 2H, CH_2), 5.53 (br. s, 2H, NH_2), 5.81 (t, J = 6, 1H, NH), 6.89 (d, J = 9, 2H, p-methoxybenzyl), 6.96 (br. s, 3H, NH_2, CH quinazoline), 7.03 (m, 2H, CH quinazoline), 7.35 (d, J = 9, 2H, p-methoxybenzyl); ^{13}C NMR (DMSO-d_6): 46.69 (CH_2), 55.45 (CH_3–O), 100.89 (CH, quinazoline), 111.15 (C, quinazoline), 114.02 (CH, p-methoxybenzyl), 123.91 (CH, quinazoline), 125.35 (CH, quinazoline), 129.42 (CH, p-methoxybenzyl), 132.31 (C, p-methoxybenzyl), 143.26 (C–NH, quinazoline), 145.37 (C, quinazoline), 158.57 (C–O, p-methoxybenzyl), 158.70 (C–NH_2, quinazoline), 161.85 (C–NH_2, quinazoline). MS (+FAB) m/z = 296 (M+1); HRMS (+FAB) calcd for $C_{16}H_{18}N_5O$: 296.15, found: 296.15.

4.1.3. N,N′-{6-[(4-Methoxybenzyl)amino]quinazoline-2,4-diyl} diacetamide (**2**)

A solution of 4-methoxybenzaldehyde (0.22 g, 1.61 mmol), compound **12** (0.5850 g, 2.26 mmol), acetic acid (one drop) in *N,N*-dimethylformamide (1 mL) was stirred at 85 °C for 1 h. Then the reaction mixture was cold to 0 °C and was added $NaBH_4$ (0.09 g, 2.58 mmol). Later, it was stirred at room temperature for 12 h. After the mixture was concentrated under decreased pressure and cold water was poured above it, the solid was filtered off, washed with cold water and dried.

Yellow powder (0.38 g, Yield: 45%, Mp = 187.1–188.2 °C), TLC ($CHCl_3$/MeOH, 80:20) R_f = 0.73. IR (KBr): 3324 and 3221 (N–H), 1692 and 1653 (C=O), 1574 and 1511 (C=C Ar); ^{1}H NMR (DMSO-d_6) δ: 2.18 (s, 3H, CH_3), 2.45 (s, 3H, CH_3), 3.72 (s, 3H, CH_3), 4.28 (d, J = 5.3 Hz, 2H, CH_2), 6.62 (t, J = 5.3, 1H, NH), 6.9 (d, J = 8.4, 1H, aromatic p-methoxibenzyl), 7.07 (s, 1H, aromatic quinazoline), 7.34 (d, J = 8.4 Hz, 1H, aromatic p-methoxibenzyl), 7.39 (br, 1H, 1H, aromatic quinazoline), 7.48 (s, J = 8.3, 1H, aromatic quinazoline), 10.49 (s, 1H, NH amide), 10.25 (s, 1H, NH amide); ^{13}C NMR (DMSO-d_6) δ: 24.39 and 25.22 (CH_3,amide), 46.20 (CH_2), 55.05 (O–CH_3), 98.44 (CH, quinazoline), 113.76 (CH, p-methoxybenzyl), 115.54 (C, quinazoline), 125.86 (CH, quinazoline), 127.17 (CH, quinazoline), 128.92 (CH, p-methoxybenzyl), 131.14 (C, p-methoxybenzyl), 143.49 (C–NH, quinazoline), 145.16 (C, p-methoxybenzyl) 146.30 (C, quinazoline), 149.95 (C-amide, quinazoline), 155.64 (C-amide, quinazoline), 158.31 (C–O, p-methoxybenzyl), 168.86 (C=O, amide), 171.54 (C=O, amide); MS (+FAB) m/z = 380 (M+1); HRMS (+FAB) calcd for $C_{20}H_{21}N_5O_3$: 380.17, found 380.17.

4.1.4. N^6-(2,3-Dihydro-1,4-benzodioxin-6-ylmethyl)quinazoline-2,4,6-triamine (**3**)

Yellow powder (0.33 g, 63%, Mp: 134.5–136.2 °C). TLC ($CHCl_3$/MeOH = 80/20) R_f = 0.24. IR (KBr): 3442 and 3353 (N–H), 1622 (C–N), 1567 and 1507 (C=C Ar), 1285 (C–O–C); ^{1}H NMR (DMSO-d_6) ppm: 4.15 (d., J = 6, 2H, CH_2), 4.19 (s, 4H, O–CH_2), 5.55 (br. s, 2H, NH_2), 5.86 (t, J = 6, 1H, NH), 6.78 (d, J = 8, 1H, benzodioxane), 6.86 (dd, J_1 = 2, J_2 = 8, 1H, benzodioxane), 6.92 (m, 2H, CH quinazoline, CH benzodioxane), 6.98 (br. s, 2H, NH_2), 7.02 (br. s, 2H, CH quinazoline); ^{13}C NMR (DMSO-d_6): 46.39 (CH_2), 64.02 (CH_2–O), 100.52 (CH, quinazoline), 110.76 (C, quinazoline), 116.44 (CH, benzodioxane), 116.74 (CH,benzodioxane), 120.65 (CH,benzodioxane), 123.51 (CH, quinazoline), 124.96 (CH, quinazoline), 133.20 (C, benzodioxane), 142.18 (C–O, benzodioxane), 142.79 (C–NH, quinazoline), 143.11 (C–O, benzodioxane), 144.91 (C, quinazoline), 158.32 (C–NH_2, quinazoline), 161.47 (C–NH_2, quinazoline). MS (TOF MS ES +) m/z = 324 (M+1); HRMS (TOF MS ES +)calcd for $C_{17}H_{18}N_5O_2$: 324.15, found: 324.15.

4.1.5. N^6-{4-[(Dimethylamino)propoxy]benzyl}quinazoline-2,4,6-triamine (**4**)

Yellow powder (0.29 g, 49%, Mp: 198.1–200.4 °C). TLC ($CHCl_3$/MeOH = 80/20) R_f = 0.02. IR (KBr): 3393 and 3347 (N–H), 1625 (C–N), 1568 and 1512 (C=C Ar), 1240 (C–O–C); ^{1}H NMR (DMSO-d_6) ppm: 1.80 (q, J = 7, 2H, CH_2), 2.11 (s, 6H, CH_3–N), 2.31 (t, J = 7, 2H, CH_2–N), 3.94 (t, J = 7, 2H, CH_2–O), 4.19 (d., J = 6, 2H, CH_2), 5.53 (br. s, 2H, NH_2), 5.82 (t, J = 6, 1H, NH), 6.89 (d, J = 9, 2H, aromatic p-dimethylaminopropoxybenzyl), 6.98 (br. s, 3H, NH_2, CH quinazoline), 7.03 (m, 2H, CH quinazoline), 7.32 (d, J = 9, 2H, aromatic p-dimethylaminopropoxybenzyl); ^{13}C NMR (DMSO-d_6): 27.01 (CH_2), 45.28 (CH_3–N), 46.59 (CH_2–NH),55.77 (CH_2–N), 65.77 (CH_2–O), 100.52 (CH, quinazoline), 110.79 (C, quinazoline), 114.18 (CH, aromatic p-dimethylaminopropoxybenzyl), 123.51 (CH, quinazoline), 125.01 (CH, quinazoline), 129.03 (CH, aromatic p-dimethylaminopropoxybenzyl), 131.86 (C, aromatic p-dimethylaminopropoxybenzyl), 142.90 (C–NH, quinazoline), 145.06 (C, quinazoline), 157.60 (C–O, p-dimethylaminopropoxybenzyl), 158.36 (C–NH_2, quinazoline), 161.48 (C–NH_2, quinazoline). MS (TOF MS ES +) m/z = 367 (M+1); HRMS (TOF MS ES +) calcd for $C_{20}H_{27}N_6O$: 367.22, found: 367.22.

4.1.6. N^6-(4-Trifluoromethoxybenzyl)quinazoline-2,4,6-triamine (**5**)

White powder (0.49 g, Yield: 88%, Mp = 206.1–207 °C), TLC ($CHCl_3$/MeOH, 80:20) R_f = 0.32. IR (KBr): 3444 and 3351 (N–H), 1673 (C–N), 1488 and 1567 (C=C Ar), 1266 (C–O–C), 1143 (C–F). ^{1}H NMR (DMSO-d_6) δ: 4.32 (d., J = 6, 2H, CH_2), 5.6 (br. s, 2H, NH_2), 6.05 (t, J = 6, 1H, NH), 6.97 (s, 1H, CH, quinazoline), 7.08 (br. s, 3H, CH quinazoline and NH_2), 7.28 (d., J = 8, 2H, p-trifluoromethoxibenzyl), 7.52 (d, J = 8, 2H, p-trifluoromethoxibenzyl); ^{13}C NMR (DMSO-d_6) δ: 46.55 (CH_2), 101.01 (CH, quinazoline), 111.16 (C, quinazoline), 120.53 (q, J = 257, CF_3), 121.20 (CH, p-trifluoromethoxybenzyl), 123.82 (CH, quinazoline), 125.44 (CH, quinazoline), 129.76 (CH, p-trifluoromethoxybenzyl), 140.12 (C, p-trifluoromethoxybenzyl), 143.11 (C, quinazoline), 145.27 (C, quinazoline), 147.53 (C, p-trifluoromethoxybenzyl), 147.60 (CF_3), 158.72 (C–NH_2, quinazoline), 161.94 (C–NH_2, quinazoline); MS (+FAB) m/z = 349 (M+1); HRMS (+FAB) calcd for $C_{16}H_{14}F_3N_5O$: 349.31, found 350.12.

4.1.7. N^6-Ethyl-N^6-(4-trifluoromethoxybenzyl)quinazoline-2,4,6-triamine (**6**)

A solution of acetaldehyde (0.84 mL, 14.95 mmol), compound **5** (0.31 g, 0.89 mmol) and sodium cyanoborohydride [$NaBH_3CN$] (0.26 g, 4.14 mmol) was added and subjected to constant stirring in 34 mL of acetonitrile for 2 min, then, concentrated HCl was slowly added until pH = 2. It was stirred for half hour and the reaction mixture was poured into a cold solution of sodium carbonate and then filtered to obtain the product. The solid was washed with ether, filtered and the obtained solution was concentrated to get a yellow powder. Recrystallization from methanol gave the desired product.

Pale yellow needles (0.15 g, Yield: 45%, Mp = 176.5–178.1 °C). TLC ($CHCl_3$/MeOH = 80/20) R_f = 0.35. IR (KBr): 3322 and 3158

(C–N), 1618 (C=N), 1558 and 1507 (C=C Ar), 1253 and 1155 (C–F), 1219 (C–O); ^{1}H NMR (DMSO-d_6) ppm: 1.09 (t, J = 7, 2H, CH_3), 3.41 (c, J = 7, 2H, CH_2), 4.54 (s, 2H, CH_2), 5.54 (s, 2H, NH_2), 7.06 (m, 4H, CH quinazoline and NH_2), 1.06 (d, J = 2, 1H, CH quinazoline), 7.26 (d, J = 8, 2H, CH p-trifluoromethoxibenzyl), 7.35 (d, J = 8, 2H, p-trifluoromethoxibenzyl); ^{13}C NMR (DMSO-d_6): 11.91 (CH_3 ethyl), 44.93 (CH_2 ethyl), 52.57 (CH_2), 104.25 (CH, quinazoline), 110.87 (C, quinazoline), 120.01 (q, J = 257, CF_3), 120.89 (CH, p-trifluoromethoxybenzyl), 123.82 (CH, quinazoline), 125.44 (CH, quinazoline), 129.76 (CH, p-trifluoromethoxybenzyl), 140.12 (C, p-trifluoromethoxybenzyl), 143.11 (C, quinazoline), 145.26 (C, quinazoline), 147.54 (C, p-trifluoromethoxybenzyl), 158.72 (C–NH_2, quinazoline), 161.94 (C–NH_2, quinazoline); MS (TOF MS ES +) m/z = 378 (M+1); HRMS (TOF MS ES +) calcd for $C_{18}H_{19}F_3N_5O$ 378.15, found 378.15.

4.1.8. Synthesis of compounds **7**–**9**

The amine **1** or **5** (1 mmol) and 4-methoxybenzaldehyde or 4-trifluoromethoxybenzaldehyde (5 mmol) were subjected to stirring at room temperature in 5 mL of a mixture of acetic acid and acetonitrile (1:1) with 5 mmol of sodium triacetoxyborohydride [$NaBH(OAc)_3$] for 7 days. After this time, 15 mL of methanol and sodium carbonate were added to neutralize the acetic acid. The solvent was evaporated, then the solid was redissolved in acetone, filtered and the obtained solution was subjected to flash chromatography for purification eluted with chloroform: methanol 98:2.

4.1.9. N^6,N^6-di(4-Methoxybenzyl)quinazoline-2,4,6-triamine (**7**)

Brown powder (0.096 g, 23%, Mp: 106.1–107.4 °C). TLC ($CHCl_3$/MeOH = 80/20) R_f = 0.43. IR (KBr): 3329 and 3147 (N–H), 1655 (C=N), 1509 (C=C Ar), 1242 (C–O–C); ^{1}H NMR (DMSO-d_6) ppm: 3.70 (s, 6H, CH_3), 4.51 (s, 4H, CH_2), 6.35 (br. s, 2H, NH_2), 6.85 (d, J = 9, 4H, CH p-methoxybenzyl), 7.11 (d, J = 9, 1H, CH quinazoline), 7.17 (d, J = 9, 4H, CH p-methoxybenzyl), 7.21 (dd, J_1 = 9, J_2 = 3, 1H, CH quinazoline), 7.36 (d, J = 3, 1H, CH quinazoline), 7.55 (br. s, 2H, NH_2); ^{13}C NMR (DMSO-d_6): 53.10 (CH_2), 55.01 (O–CH_3), 105.45 (CH, quinazoline), 110.47 (C, quinazoline), 113.77 (CH, p-methoxybenzyl), 114.53 (CH, quinazoline), 122.33 (CH, quinazoline), 122.87 (CH, quinazoline), 128.56 (CH, p-methoxybenzyl), 130.44 (C, p-methoxybenzyl), 140.39 (C, quinazoline), 143.86(C–NH, quinazoline), 157.14(C–NH_2, quinazoline), 158.19 (C–O, p-methoxybenzyl), 161.98 (C–NH_2, quinazoline). MS (+FAB) m/z = 416 (TOF MS ES +); HRMS (TOF MS ES +) calcd for $C_{24}H_{25}N_5O_2$: 416.21, found: 416.21.

4.1.10. N^6-(4-Methoxybenzyl)-N^6-(4-trifluoromethoxybenzyl) quinazoline-2,4,6-triamine (**8**)

Yellow powder (0.30 g, 63%, Mp: 120.8–121.9 °C). TLC ($CHCl_3$/MeOH = 80/20) R_f = 0.40. IR (KBr): 3390 and 3157 (N–H), 1682 (C–N), 1555 and 1511 (C=C Ar), 1322 (C–F), 1243 (C–O–C); ^{1}H NMR (DMSO-d_6) ppm: 3.69 (s, 3H, CH_3), 4.57 (s, 2H, CH_2), 4.63 (s, 2H, CH_2), 6.49 (br. s, 2H, NH_2), 6.85 (d, J = 9, 2H, p-methoxybenzyl), 7.12 (d, J = 9, 1H, CH quinazoline), 7.19 (d, J = 9, 1H, CH p-methoxybenzyl),7.20 (dd, J_1 = 9, J_2 = 3, 1H, CH quinazoline), 7.28 (d, J = 9, 2H, CH p-trifluoromethoxybenzyl), 7.36 (m, 3H, CH p-trifluoromethoxybenzyland CH quinazoline), 7.63 (br. s, 2H, NH_2); ^{13}C NMR (DMSO-d_6): 52.85 (CH_2), 53.40 (CH_2), 55.02 (O–CH_3), 105.13 (CH, quinazoline), 110.47 (C, quinazoline), 113.83 (CH, p-methoxybenzyl), 120.11 (q, J = 257, CF_3), 121.03 (CH, p-trifluoromethoxybenzyl), 122.16 (CH, quinazoline), 122.44 (CH, quinazoline), 128.52 (CH, p-methoxybenzyl), 128.94 (CH, p-trifluoromethoxybenzyl),130.24 (C, p-methoxybenzyl), 138.01(C, quinazoline),138.43 (C, p-trifluoromethoxybenzyl), 143.64 (C–NH, quinazoline), 147.14 (C, p-trifluoromethoxybenzyl), 156.90 (C–NH_2, quinazoline), 158.25 (C–O, p-methoxybenzyl), 162.02 (C–NH_2, quinazoline). MS (TOF MS ES +) m/z = 470 (M+1); HRMS (TOF MS ES +) calcd for $C_{24}H_{23}N_5O_2F_3$: 470.18, found: 470.18.

4.1.11. N^6,N^6-di(4-Trifluoromethoxybenzyl)quinazoline-2,4,6-triamine (**9**)

Orange powder (0.18 g, 34%, Mp: 132.9–134.7 °C). TLC ($CHCl_3$/MeOH = 80/20) R_f = 0.36. IR (KBr): 3331 and 3217 (N–H), 1630 (C–N), 1527 and 1416 (C=C Ar), 1320 (C–F), 1160 (C–O–C); ^{1}H NMR (DMSO-d_6) ppm: 4.69 (s, 4H, CH_2), 6.62 (br. s, 2H, NH_2), 7.14 (d, J = 9, 1H, CH quinazoline), 7.19 (dd, J_1 = 9, J_2 = 2, 1H, CH quinazoline), 7.29(d, J = 8, 4H, CH p-trifluoromethoxybenzyl), 7.37 (d, J = 8, 4H, CH p-trifluoromethoxybenzyl), 7.38 (s, 1H, CH quinazoline), 7.69 (br. s, 2H, NH_2); ^{13}C NMR (DMSO-d_6): 53.17 (CH_2), 105.19 (CH, quinazoline), 110.91 (C, quinazoline), 120.51 (c, J = 257, CF_3), 121.46 (CH, p-trifluoromethoxybenzyl), 121.82 (CH, quinazoline), 122.39 (CH, quinazoline), 129.31 (CH, p-trifluoromethoxybenzyl), 138.67 (C, p-trifluoromethoxybenzyl), 143.79 (C, quinazoline), 143.82 (C, quinazoline), 147.60 (C, p-trifluoromethoxybenzyl), 157.27 (C–NH_2, quinazoline), 162.43 (C–NH_2, quinazoline). MS (TOF MS ES +) m/z = 522 (M+1); HRMS (TOF MS ES +) calcd for $C_{24}H_{18}N_5O_2F_6$: 522.14, found: 522.17.

4.1.12. 6-Nitroquinazoline-2,4-diamine (**11**)

Sodium hydroxide (3.4 g, 85 mmol) was added to a solution of guanidine hydrochloride (3.65 g, 38 mmol) in ethanol, and the reaction was stirred for 20 min at room temperature. The solution was then stirred under reflux for 6 h with 5-nitroanthranilonitrile (5 g, 31 mmol) in 1-propanol (40 mL). Then, the mixture was cooled to 0 °C. The solid was filtered off, washed with cold water, washed with cold ethanol and dried. An orange solid product was obtained (5.4 g, 86%, Mp: 360 °C), TLC (2-butanol/acetic acid/water = 80/20/5) R_f = 0.4. IR (KBr): 3464 and 3440 (N–H), 1614 (C–H, aromatic), 1325 (NO_2). ^{1}H NMR (DMSO-d_6): 6.77 (s, 2H, NH_2), 7.22 (d, J = 9, 1H, aromatic), 7.86 (s, 2H, NH_2), 8.21 (dd, J_1 = 3, J_2 = 9, 1H, aromatic), 9.08 (d, J = 3, 1H, aromatic); ^{13}C NMR (DMSO-d_6): 108.84, 121.92, 124.87, 126.63, 139.12, 157.28, 163.00, 163.025. Anal. Calcdfor $C_{12}H_{13}N_5O_2$: C, 46.83; H, 3.44; N, 34.13.

4.1.13. N-[2-(Acetylamino)-6-aminoquinazolin-4-yl]acetamide (**12**)

Compound **3** (1 g, 4.87 mmol) and acetic anhydride (1 mL) were heated at 100° C for 12 h. Then, the reaction mixture was poured into cold water, and the solid was filtered off, washed with cold water at pH 7 and dried. A yellow solid (**3a**) was obtained (0.89 g, 65%, Mp: 278 °C), TLC ($CHCl_3$/MeOH = 60/40) R_f = 0.8. Anal. Calcd for $C_{12}H_{11}N_5O_4$: C, 49.83; H, 3.83; N, 24.21. Found: C, 49.99; H, 3.11; N, 23.81.

The catalytic reduction of **3a** (0.5 g, 1.73 mmol) with hydrogen and Pd/C (10%) (0.05 g) was performed on a Parr assembly at 60 psi at room temperature for 1 h. The catalyst was then removed by filtration, and the filtrate was concentrated on a rotavapor under reduced pressure to yield **4** (0.34 g, 76%, Mp = 238 °C), TLC ($CHCl_3$/MeOH = 60/40) R_f = 0.67. IR (KBr): 3353 and 3230 (N–H). ^{1}H NMR (DMSO-d_6): 2.2 (s, 3H, CH_3), 2.34 (s, 3H, CH_3), 5.61 (br. s, 2H, NH_2), 7.04 (d, J = 3, 1H, aromatic), 7.28 (dd, J_1 = 8, J_2 = 3, 1H, aromatic), 7.5 (d, J = 8, 1H, aromatic), 10.46 (br. s, 1H, NH amide), 10.22 (br. s, 1H, NH amide); ^{13}C NMR (DMSO-d_6): 24.51, 102.37, 116.82, 126.02, 127.48, 145.16, 146.55, 150.08, 156.08, 169.18, 170.73. Anal. Calcd for $C_{12}H_{13}N_5O_2$: C, 55.59; H, 5.05; N, 27.01. Found:C, 57.0; H, 4.52; N, 25.20.

4.2. In vitro trypanocidal assays

Two mexican strains of *T. cruzi* (INC-5 and NINOA) were used. The parasites were maintained in the laboratory in the vector *Meccuspallidipennis* (Insecta: Hemiptera) and by successive passages in NIH female mice of 25–30 g. INC-5 strain was obtained

from a chronic case of Chagas disease in the city of Guanajuato, Mexico; a NINOA strain was obtained from an acute case of Chagas disease by xenodiagnosis in the city of Oaxaca, Mexico [16]. The test was evaluated in vitro on bloodstream trypomastigotes of both strains. Blood was obtained by cardiac puncture of a female NIH mice at the peak of parasitaemia (4×10^6 parasites/mL). Heparin was used as anticoagulant. Infected blood was diluted with a 0.85% sterile saline solution to a final concentration of 1×10^6 trypomastigotes/mL. For each compound, stock was prepared in dimethyl sulfoxide (DMSO) (10 mg/mL). Then, each stock solution was serially diluted in sterile distilled water to the desired concentration. For the in vitro assay, sterile 96-well culture plates were used. Each plate contained 195 μL of the suspension of bloodstream trypomastigotes and 5 μL of each dilution so that each compound was evaluated at a final concentration of 100, 50, 10 and 5 μg/mL. As a control we used a final concentration of DMSO 1% since it has been found that concentrations <5% have no impact on mobility, infectivity and ultrastructural morphology. The **Nfx**, **Bzn** and **Pyr** were used as reference compounds. The concentrations of each compound were evaluated in triplicate. The plates were incubated at 4° C for 24 h. Trypanocidal activity was evaluated by counting the number of bloodstream trypomastigotes after the incubation time by the Brener Method [17,18]. Briefly, 5 μL of blood were placed on slides, covered with a coverslip and the flagellates were examined with an optical microscope at 40× magnification. Trypanocidal activity was expressed in terms of lysis of the flagellates after incubation time compared with the control group. The IC_{50} (mM) was calculated using the program GraphPadPrism®.

4.3. Antileishmania assays

The antileishmanial activity was tested in an in vitro culture of the *L. mexicana* strain MHOM/BZ/61/M379 growing in Dulbecco's modified Eagle's medium (DMEM) containing L-glutamine and glucose (4.5 mg/L), without sodium bicarbonate (GIBCO, Grand Island, NY), supplemented with 10% fetal calf serum (GIBCO) [19,20]. The experiments were performed in 24-well plates for tissue culture by adding 0.5 mL of one of the serial dilutions of the compound solubilized in a specified solvent (in a ratio of 1:10 of compound:media) to each well along with 0.5 mL 2×10^6 parasites/mL. The plates were stored at 26 °C for 24 h. The parasite density was counted with a hemacytometer in triplicate. The presented results are expressed in terms of the LC_{50} (50% lytic concentration).

4.4. Cytotoxicity studies

From a bottle (t-25) with 100% of cell confluence, we performed a cell suspension (cells were washed with 1× PBS, trypsinized (trypsin 0.25%) and MEM culture medium added 10% FBS). In a 96-well microplate, 100 μL of cell suspension were placed in each of the rows. In the microplates, they were incubated at 37° C in a humid atmosphere with 5% CO_2 for 24 h. After incubation, each well was placed in the compounds at different concentrations, using cell rows to witness DMSO, and incubated 24 h at 37° C with 5% CO_2. At the end of incubation, 50 μL of MTT solution were placed in each well of the microplate and the cells were incubated again for 2 h. 100 μL of SDS-HCl solution were added to each well. They were mixed and incubated at 24 °C, overnight. The microplate was read using an ELISA reader at a wavelength of 540 nm. Finally, we determined the viability percentage. The viability percentage was determined as follows:

$$\text{Viability } \% = (\text{OJ-treated cells/OD control cells}) \times 100$$

Each test was performed in triplicate with positive and negative controls with untreated cells, which should give an OD reading of 1 or more. The presented results are expressed in terms of the CC_{50} (50% cytotoxic concentration).

4.5. In vivo antimalarial assays

From a cryopreserved stock of *P. berghei* the contents of the vial in 3 female CD1 mice were thawed and then proceeded to inoculate initiating the transmission cycle in the mouse. Five days later, the parasitemia was determined and the mouse that had closer to 30% (30% of the erythrocytes are parasitized) had 45 drops of blood extracted from the vein, which were diluted with 2 mL of physiological saline. 0.2 mL of the diluted blood were administered intraperitoneally (ip) to 5 healthy mice. The parasitemia of this new group was revised from the second day. When parasitemia reached 30%, blood from the tail was extracted and diluted with physiological saline and 0.2 mL were administered ip to a new group of five healthy mice. This procedure was repeated until the infection was stabilized. After reaching this stabilization, we proceeded to carry out suppression tests during 4 days.

Mice were treated orally by administration of compounds (50 mg/kg) every 24 h on day 0–4 post inoculation (n = 5 in duplicate). At day 4, at about the same time that the infection was performed, blood samples from the tail vein of mice were taken, the parasitemia was determined. The inhibitory rate of the compound at day 4 was expressed as [(Parasitaemia in control group—Parasitaemia in compound treated group)/(Parasitaemia in control placebo group)] × 100%. Inhibitory rate and survival—time is recorded in comparison to untreated groups. Mice still without parasitemia on day 30 post infection are considered cured [21]. The control consisted of 0.2 mL of Arabic Gum orally administered. Positive control drugs were chloroquine (**CQ**) and pyrimethamine (**Pyr**).

4.6. ABTS assay

Experiments were performed based on the work of Re et al. with some modifications [22]. ABTS and potassium persulfate were dissolved in distilled water to a final concentration of 7 mM and 2.45 mM, respectively. These two solutions were mixed and the mixture was allowed to stand in the dark at room temperature for 16 h before use in order to produce ABTS radical ($ABTS^{\bullet+}$). For the study of compounds, the ABTS radical solution was diluted with distilled water to an absorbance of 1.00 at 734 nm. Compounds or Trolox standards (final concentrations 0–20 mM) were added to diluted $ABTS^{\bullet+}$ solution and the absorbance reading was taken 10 min after mixing using the spectrophotometer. Results are presented as the ability of compounds to scavenge 50% of free radical $ABTS^{\bullet+}$ (IC_{50}). Parameters IC_{50} (μM) were determined with a relative uncertainty of less than five percent.

4.7. DHFR inhibition

DHFR inhibition effect was tested on the in vitro growth assay for promastigotes of *L. mexicana* [23]. The evaluated concentrations of compounds **5** and **6** on the leishmania parasites were of 8 μM and 3 μM, respectively. To test DHFR inhibition by folinic acid, folic acid and ferulic acid, the compounds were incubated with 20, 40, 60, 80 or 100 μM with 10^6 leishmania at the logarithmic phase of growth, washed and resuspended with PBS and incubated for 1 h at room temperature. Then, the parasites were centrifuged, the media was eliminated, and the parasites were resuspended in the culture media and distributed in a 24-well plate. Compounds were then added at the desired concentration, and the plates were incubated for 24 h. The percentage of living parasites was calculated using the

formula % AP = 100 × (*Tc* − *Tp*)/*Tc*, where % AP is the percentage of growth inhibition for each period, each dosage, *Tc*, is the number of parasites/mL in the control wells, and *Tp* is the average number of moving parasites/mL.

4.8. Modeling

Molecular modeling was performed with **NAMD 2.6**, **Modeler**, **Gaussian 03**, **Autodock 4.0.1** and **VMD** programs [24–27]. The DHFR proteins were obtained from Protein Data Bank (PDB) (ID-PDB: 2H2Q, 2BL9 and 1KMS from *T. cruzi*, *P. vivax* and human, respectively). To construct DHFR *L. major*, the *T. cruzi* enzyme (ID-PDB: 2H2Q Key) was used as the template. First, the amino acids were corrected with the Modeler program. Classical MD simulations were performed using the NAMD 2.6 program with the CHARMM27 force field, and water molecules were added using the VMD program. The structure was neutralized with 4 sodium ions after being immersed in a TIP3P water box containing 9249 water molecules. The equilibration protocol began with 1500 minimization steps followed by 30 ps of MD at 310 K with fixed protein atoms. Then, the entire system was minimized to 1500 steps (at 0 K) and then heated gradually from 10 to 310 K by temperature reassignment during the first 60 ps of 100 ps equilibration dynamics without restraints. The final step was a 30 ps NTP dynamics using the Nose-Hoover Langevin piston pressure control 28 at 310 K and 1.01325 bar for density (volume) fitting. From this point, the simulation continued in the NTV ensemble for 5 ns. The periodic boundary conditions and the particle-mesh Ewald method were applied for a complete electrostatics calculation. The dielectric water constant was used, and the temperature was maintained at 310 K using Langevin dynamics. The structure was allowed to converge, which was reached at 10 ns. A snapshot was obtained at this time for computational docking. Docking was also performed for PTR from *L. major* and *T. cruzi* (ID-PDB: 1WOC and1MXF, respectively). The structure for lmPTR1, which was obtained after crystallization with **TAQ**, validated the study.

For docking of all proteins, water molecules were removed and its active site was defined as all residues within a grid of 120 Å × 120 Å × 120 Å with a center in the protein for blind docking and then within a grid of 60 Å × 60 Å × 60 Å to 6.5 Å centered at coordinates XYZ for focused docking, with an initial population of 100 randomly placed individuals and a maximum number of 1.0×10^7 energy evaluations. The compounds for docking were drawn in Gauss view 3.0. Before docking, the compounds were subjected to a conformational analysis and energy minimization using the hybrid functional B3LYP with a set of bases 6, 31 G(d,p). Docking studies were made with three minimum energy conformations for evaluation of conformational space. The values of Kd and ΔG were taken of conformation with minimum energy and large K_d have been reported elsewhere. This study was validated, also compared the conformation of **Pyr** between crystalline structure and docking result satisfactorily. The proteins pvDHFR and lmDHFR were used like *P. berghei* and *L. mexicana* models, respectively. The physicochemical properties were calculated with **ACD/ChemSketh**. The graphics were prepared with **OriginLab** and figures with **ACD/ChemSketh** (for structures) and **PyMOL** (proteins and ligands).

Acknowledgments

This study was supported by fellowship and infrastructure purchased with funds from PAPIIT-UNAM IN213914, and funds research from CONACYT-62488 and SIT/COFAA-IPN. We are grateful to Rosa Isela del Villar, Georgina Duarte, Margarita Guzmán, Nayeli López and Marisela Gutiérrez from Facultad de Química-USAI, UNAM, for the determination of all spectra. For theoretical studies we are grateful to DGSCA-UNAM for allowing us the use of Kan-Balam supercomputer.

Appendix A. Supplementary data

Supplementary data related to this article can be found at http://dx.doi.org/10.1016/j.ejmech.2015.04.028.

References

[1] K.T. Andrews, G. Fisher, T.S. Skinner-Adams, Drug repurposing and human parasitic protozoan diseases, Int. J. Parasitol. Drugs Drug Resist. 4 (2014) 95–111, http://dx.doi.org/10.1016/j.ijpddr.2014.02.002.

[2] C.J. Perez, A.J. Lymbery, R.C.A. Thompson, Chagas disease: the challenge of polyparasitism, Trends Parasitol. 30 (2014) 176–182, http://dx.doi.org/10.1016/j.pt.2014.01.008.

[3] R.M. Reguera, E. Calvo-Álvarez, R. Álvarez-Velilla, R. Balaña-Fouce, Target-based vs. phenotypic screenings in Leishmania drug discovery: a marriage of convenience or a dialogue of the deaf? Int. J. Parasitol. Drugs Drug Resist. (2014) http://dx.doi.org/10.1016/j.ijpddr.2014.05.001.

[4] S. Mandal, Epidemiological aspects of vivax and falciparum malaria: global spectrum, Asian Pac. J. Trop. Dis. 4 (Suppl. 1) (2014) S13–S26, http://dx.doi.org/10.1016/S2222-1808(14)60410-2.

[5] G. Valencia-Pacheco, E. Nalleli Loría-Cervera, E.I. Sosa-Bibiano, E.B. Canché-Pool, A. Vargas-Gonzalez, P.C. Melby, F.J. Andrade-Narvaez, In situ cytokines (IL-4, IL-10, IL-12, IFN-c) and chemokines (MCP-1, MIP-1a) gene expression in human Leishmania (Leishmania)mexicana infection, Cytokine 69 (2014) 56–66, http://dx.doi.org/10.1016/j.cyto.2014.05.016.

[6] A.R. Renslo, J.H. McKerrow, Drug discovery and development for neglected parasitic diseases, Nat. Chem. Biol. 212 (2006) 701–710.

[7] (a) J.A. Urbina, R. Docampo, Specific chemotherapy of Chagas disease: controversies and advances, Trends Parasitol. 19 (2003) 495–501;
(b) A.A. Mielniczki-Pereira, C.M. Chiavegatto, J.A. López, W. Colli, M.J.M. Alves, F.R. Gadelha, *Trypanosoma cruzi* strains, Tulahuen 2 and Y, besides the difference in resistance to oxidative stress, display differential glucose-6-phosphate and 6-phosphogluconate dehydrogenases activities, Acta Trop. 101 (2007) 54–60;
(c) R.L. Cardoni, M.T. Rimoldi, M.M.E. de Bracco, *Trypanosoma cruzi*: Nifurtimox's effect on infectivity, Exp. Parasitol. 43 (1977) 370–375.

[8] S. LCroft, G.H. Coombs, Leishmaniasis-current chemotherapy and recent advances in the search for novel drugs, Trends Parasitol. 19 (2003) 502–508.

[9] Reviews on chemotherapeutics against malaria, see: (a) J. Wiesner, R. Ortmann, H. Jomaa, M. Schlitzer, New antimalarial drugs, Angew. Chem. Int. Ed. 42 (2003) 5274–5293;
(b) M. Schlitzer, Malaria chemotherapeutics part I: history of antimalarial drug development, currently used therapeutics, and drugs in clinical development, ChemMedChem 2 (2007) 944–986;
(c) A. Nzila, The past, present and future of antifolates in the treatment of *Plasmodium falciparum* infection, J. Antimicrob. Chemother. 57 (2006) 1043–1054;
(d) A. Attaran, K.I. Barnes, C. Curtis, U. d'Alessandro, C.I. Fanello, M.R. Galinski, G. Kokwaro, S. Looareesuwan, M. Makanga, T.K. Mutabingwa, A. Talisuna, J.F. Trape, W.M. Watkins, WHO, the Global Fund, and medical malpractice in malaria treatment, Lancet 363 (2004) 237–240.

[10] J. Davoll, A.M. Johnson, H.J. Davies, O.D. Bird, J. Clarke, E.F. Elslager, 2,4-Diamino-6-{[aralkyl and (heterocyclic)methyl]amino}quinazolines, a novel class of antimetabolites of interest in drug-resistant malaria and Chagas' disease, J. Med. Chem. 15 (1972) 812–826.

[11] K. McLuskey, F. Gibellini, P. Carvalho, M.A. Avery, W.N. Hunter, Inhibition of *Leishmania major* pteridine reductase by 2,4,6-triaminoquinazoline: structure of the NADPH ternary complex, Acta Crystallogr. Sect. D. 60 (2004) 1780–1785.

[12] J.D. Berman, M. King, N. Edwards, Antileishmanial activities of 2,4-diaminoquinazoline putative dihydrofolate reductase inhibitors, Antimicrob. Agents Chemother. 33 (1989) 1860–1863.

[13] S. Khabnadideh, D. Pez, A. Musso, R. Brun, L.M. Ruiz-Perez, D. Gonzalez-Pacanowska, I.H. Gilbert, Design, synthesis and evaluation of 2,4-diaminoquinazolines as inhibitors of trypanosomal and leishmanial dihydrofolate reductase, Bioorg. Med. Chem. 13 (2005) 2637–2649.

[14] B. Nare, L.W. Hardy, S.M. Beverley, The roles of pteridine reductase 1 and dihydrofolate reductase-thymidylate synthase in pteridine metabolism in the protozoan parasite Leishmania major, J. Biol. Chem. 272 (1997) 13883–13891.

[15] C. Robello, P. Navarro, S. Castanys, F. Gamarro, A pteridine reductase gene ptr1 contiguous to a P-glycoprotein confers resistance to antifolates in Trypanosoma cruzi, Mol. Biochem. Parasitol. 90 (1997) 525–535.

[16] M.F. Bosseno, C. Barnabé, E.M. Gastélum, F.L. Kasten, J. Ramsey, B. Espinoza, S.F. Brenière, Predominance of *Trypanosoma cruzi* lineage I in Mexico, J. Clin. Microbiol. 40 (2002) 627–632.

[17] W. Raether, R. Michel, M. Uphoff, Effects of dimethylsulfoxide and the deep-freezing process on the infectivity, motility, and ultrastructure of

Trypanosoma cruzi, Parasitol. Res. 74 (1988) 307–313.
[18] (a) Z. Brener, Therapeutic activity and criterion of cure on mice experimentally infected with *Trypanosoma cruzi*, Rev. Inst. Trop. Paulo 4 (1962) 389–396;
(b) L.S. Filardi, Z. Brener, A rapid method for testing in vivo the susceptibility of different strains of *Trypanosoma cruzi* to active chemotherapeutic agents, Mem. Inst. Oswaldo Cruz 79 (1984) 221–225.
[19] H. Martinez-Rojano, J. Mancilla-Ramirez, L. Quiñonez, N. Galindo-Sevilla, Activity of hydroxyurea against *Leishmania mexicana*, Antimicrob. Agents Chemother. 52 (2008) 3642–3647.
[20] L. Quiñonez-Díaz, J. Mancilla, M. Avila-García, J. Ortíz-Avalos, A. Berron, S. Gonzalez, Y. Paredes, N. Galindo-Sevilla, Effect of ambient temperature on the clinical manifestation of experimental diffuse cutaneous leishmaniasis in a rodent model, Vector Borne Zoonotic Dis. 12 (2012) 851–860.
[21] D.A. Fidock, P.J. Rosenthal, S.L. Croft, R. Brun, S. Nwaka, Antimalarial drug discovery: efficacy models for compound screening, Nat. Rev. Drug Discov. 3 (2004) 509–520.
[22] R. Re, N. Pellegrini, A. Proteggente, A. Pannala, M. Yang, C. Rice-Evans, Antioxidant activity applying an improved ABTS radical cation decolorization assay, Free Radic. Biol. Med. 26 (1999) 1231–1237.
[23] S. Bag, N.R. Tawari, R. Sharma, K. Goswami, M.V.R. Reddy, M.S. Degani, In vitro biological evaluation of biguanides and dihydrotriazines against Brugia malayi and folate reversal studies, Acta Trop. 113 (2010) 48–51.
[24] J.C. Phillips, R. Braun, W. Wang, J. Gumbart, E. Tajkhorshid, E. Villa, C. Chipot, R.D. Skeel, L. Kale, K. Schulten, Scalable molecular dynamics with NAMD, J. Comput. Chem. 26 (2005) 1781–1802.
[25] A. Sali, T.L. Blundell, Comparative protein modelling by satisfaction of spatial restraints, J. Mol. Biol. 234 (1993) 779–815.
[26] G.M. Morris, R. Huey, W. Lindstrom, M.F. Sanner, R.K. Belew, D.S. Goodsell, A.J. Olson, Autodock4 and AutoDockTools4: automated docking with selective receptor flexibility, J. Comput. Chem. 16 (2009) 2785–2791.
[27] W. Humphrey, A. Dalke, K. Schulten, VMD – visual molecular dynamics, J. Molec. Graph. 14 (1996) 33–38.